JOURNAL OF AIRCRAFT
Vol. 48, No. 1, January–February 2011

Bilevel Optimization of Blended Composite Wing Panels

Dianzi Liu,* Vassili V. Toropov,† Osvaldo M. Querin,‡ and David C. Barton§
University of Leeds, Leeds, England LS2 9JT, United Kingdom

DOI: 10.2514/1.C000261

Two approaches are examined for finding the best stacking sequence of laminated composite wing structures with blending and manufacturing constraints: smeared-stiffness-based method and lamination-parameter-based method. In the first method, the material volume is the objective function at the global level, and the stack shuffling to satisfy blending and manufacturing constraints is performed at the local level. The other method introduced in this paper is to use lamination parameters and numbers of plies of the predefined angles (0, 90, 45, and −45 deg) as design variables with buckling, strain, and ply percentage constraints while minimizing the material volume in the top-level optimization run. Given lamination parameters from the top-level optimization as targets for the local level, an optimal stacking sequence is determined to satisfy the global blending requirements. On a benchmark problem of an 18-panel wing box, the results from these two approaches are compared to published results to demonstrate their potential.

Nomenclature

$\mathbf{A}$	=	in-plane stiffness matrix
$\mathbf{D}$	=	out-of-plane stiffness matrix
E_j	=	Young's modulus in the direction j, $j = 1, 2$
F	=	point load acting on the wing box
G_{12}	=	shear modulus
h	=	thickness of a laminated panel
i	=	panel number
$N_{\max}$	=	maximum number of plies of the same angle placed sequentially in the stacking sequence
n	=	number of plies
$\bar{Q}_{ij}$	=	items in the transformed reduced-stiffness matrix, $i, j = 1, 2, 6$
t	=	ply thickness
U_i	=	material invariants, $i = 1, 2, \ldots, 5$
$\mathbf{V}$	=	vector of lamination parameters
z	=	distance of the ply position from the laminate midplane
γ_{12a}	=	allowable shear strain
ε_{ja}	=	allowable strain, $j = 1, 2$
θ	=	ply angle
ν	=	Poisson's ratio
ρ	=	material density

I. Introduction

THE material volume and the stacking sequence of plies in a composite aircraft structure are of vital importance for achieving the material's required mechanical characteristics such as in-plane, flexural, and buckling behavior [1–4]. Because of the industrial requirements and practical manufacturing considerations, symmetric and balanced laminates with ply orientations of 0, 90, 45, and −45 deg are investigated in this work.

A bilevel (global and local) strategy for optimization of a composite wing box structure was presented in [5]. At the global level, continuous optimization of thicknesses of 0, 90, 45, and −45 deg plies was performed to minimize the material volume of a wing box subject to strain and buckling constraints. For a given the number of plies of each orientation and in-plane loads, a permutation genetic algorithm (permGA) was used at the local level to optimize the stacking sequence in order to maximize the buckling load. The optimum buckling load, which was treated as a function of the loading and the numbers of plies of 0, 90, 45, and −45 deg orientation, was evaluated by a cubic polynomial response surface approximation. A similar approach was used in [6] for maximization of buckling load of composite panels.

The use of lamination parameters is another approach to represent the in-plane and flexural stiffness in the optimization of laminated composites. It was first used in [7] and later applied to the buckling optimization of orthotropic laminated plates in [8]. In [9–11] lamination parameters were used for tailoring mechanical properties of laminated composites. In a laminated composite optimization problem, lamination parameters can be used as design variables instead of layer thicknesses and ply angles in order to avoid falling into local optima. A variational approach was used to determine feasible regions in the space of lamination parameters as constraints in the optimization problem in [12].

In [13], a gradient-based optimization technique and a genetic algorithm (GA) were applied to optimize anisotropic laminated composite panels with T-stiffeners. In the first step, weight optimization based on mathematical programming was performed, in which the skin and a stiffener were parameterized using lamination parameters, subject to the constraints on buckling, strain as well as practical design rules. A composite layup of a panel was determined using a GA in the second level by meeting the target values of lamination parameters coming from the top level. In [14,15], the same approach was used for optimization of laminated composite panels with T-stiffeners, but with a different objective function at the local level that is the maximum value of the linearized design constraints. Bilevel strategy for composite layup optimization using lamination parameters can also be found in [16].

Ply compatibility (also referred to as blending) between adjacent panels is a very important consideration in the design of composite structures and the blending methodology was first introduced in [17] to ensure that a laminated composite panel was manufacturable. Later, the blending requirement has been considered in [18–23]. The composition continuity and the stacking-sequence continuity measures were defined in [18] and applied in an optimization process, also in [24]. The concepts of sublaminates (plies shared between several panels) and design variable zones (groups of panels covered by the same sublaminates) were introduced in [19] for blended panel optimization. This approach kept the total thickness of each panel obtained in the first (global) optimization step (with a margin of two to four plies) but redefined the stack composition for the sublaminates in the second (local) optimization step. Later, two

Received 15 January 2010; revision received 8 April 2010; accepted for publication 9 April 2010.

*Ph.D. Student, School of Mechanical Engineering. Student Member AIAA.
†Professor of Aerospace and Structural Engineering, School of Mechanical Engineering and School of Civil Engineering. Associate Fellow AIAA.
‡Senior Lecturer, School of Mechanical Engineering. Senior Member AIAA.
§Professor of Solid Mechanics, School of Mechanical Engineering.

blending methods, inward and outward blending, were developed in [20] to improve the ply continuity between adjacent panels using a guide based GA. An attempt to obtain global ply continuity using a stacking-sequence table (tabular method) was made in [22]. A sublaminate was repeatedly used as a stacking template for local level (laminate level) panel design, whereas laminate percentages were specified as 50% for plies of 0 deg, 40% for ±45 deg, and 10% for 90 deg in the top-level (panel level) optimization. Recently, a new approach [23] was developed to identify a laminate stacking sequence in individual wing panels satisfying interpanel continuity constraints. In this method, a conventional stacking-sequence identification problem was transformed into a problem of shuffling of a set of global ply layout cards. A permutation GA was applied to find an optimal card sequence, which uses the ply angle percentages and the chordwise and spanwise laminate thickness distributions as input data. The authors' conclusion was that it allowed to considerably reduce the design space and hence the solution time.

In this paper, two optimization approaches are used for the optimization of stacking sequence of laminated composite structures: a smeared-stiffness-based method and a lamination-parameter-based method. In the smeared-stiffness-based method, a gradient-based optimization is used to optimize the total volume of the structure at the top level subject to the buckling and strain constraints. A blending scheme and a ply shuffling code based on the layup design rules are applied. In the lamination-parameter-based method, the total number of plies and the lamination parameters related to the out-of-plane stiffness matrix are treated as the design variables in the top-level optimization problem. Buckling and strain constraints are applied at this level and the total material volume is the objective function. Next, a permutation GA is used to shuffle the layers to minimize the difference between the values of computed lamination parameters for a current stacking sequence and those coming from the top level. This is embedded into a blending procedure applied at this level to achieve the global ply continuity.

II. Optimization Strategies

Industrial requirements and practical manufacturing considerations lead to the assumption that only symmetric and balanced laminates with ply orientations 0, 90, 45, and −45 deg need to be investigated. Therefore, only half the number of plies of each orientation is given in all numerical results presented in this paper. As the number of 45 deg plies (n_{45}) is always equal to the number of −45 deg plies (n_{-45}) for balanced laminates, the number of pairs of ±45 deg plies is presented as n_{45}. At the local level, maximization of ply compatibility will be achieved by the optimization of the ply stacking sequence, whereas the laminate thickness remains constant as it is fixed after the top-level optimization.

A. Smeared Stiffness-Based Method

Smeared stiffness-based method is an approach that aims at neutralizing the stacking-sequence effects on the buckling performance by considering homogeneous sections with quasi-isotropic layups. This method is used to calculate the matrices **A** and **D** of laminates without determining a stacking sequence. Hence, no predefined stacking sequence of plies is needed in the top-level material volume optimization. According to the classical laminate theory [25], the matrices **A** and **D** can be formulated as

$$\mathbf{A} = \begin{bmatrix} A_{11} & A_{12} & A_{16} \\ & A_{22} & A_{26} \\ \text{sym} & & A_{66} \end{bmatrix}, \qquad \mathbf{D} = \begin{bmatrix} D_{11} & D_{12} & D_{16} \\ & D_{22} & D_{26} \\ \text{sym} & & D_{66} \end{bmatrix} \tag{1}$$

where

$$A_{ij} = \int_{-h/2}^{h/2} \bar{Q}_{ij}\,\mathrm{d}z, \qquad i = j = 1, 2, 6, \quad \text{and}$$

$$D_{ij} = \int_{-h/2}^{h/2} \bar{Q}_{ij} z^2\,\mathrm{d}z, \qquad i = j = 1, 2, 6$$

The membrane stiffness matrix **A** can be rewritten as

$$\mathbf{A} = h\left(\sum_{k=1}^{N} \frac{(\bar{Q}_{ij})_k}{N}\right), \qquad i = j = 1, 2, 6 \tag{2}$$

With the assumption of material homogeneity above, the bending stiffness matrix **D** can be rewritten as

$$\mathbf{D} = \bar{Q}_{ij} \int_{-h/2}^{h/2} z^2\,\mathrm{d}z = \left(\sum_{k=1}^{N} \frac{(\bar{Q}_{ij})_k}{N}\right) \frac{h^3}{12}, \qquad i = j = 1, 2, 6 \tag{3}$$

where N is the total number of plies and h is the total thickness of the laminate. Therefore, for a homogeneous material, the relationship between **A** and **D** can be formulated as

$$\mathbf{D} = \mathbf{A}h^2/12 \tag{4}$$

The application of this approach to the concept optimization of composite structures was demonstrated in [26] and implemented in Altair's OptiStruct structural optimization and finite element (FE) simulation software [27].

In our approach, a bilevel optimization process is used. The top-level optimization problem formulation is as follows:

$$\text{Minimize} \sum_{i=1}^{n} (n_0^i + n_{45}^i + n_{90}^i) A_i t$$

where t is the ply thickness, n is the total number of panels and A_i is the area of panel i.

The design variables are the numbers of plies of each orientation n_0^i, n_{45}^i and n_{90}^i, $i = 1, \ldots, n$. The strain constraints are

$$\max \varepsilon_1^i \le \varepsilon_{1a}, \qquad \max \varepsilon_2^i \le \varepsilon_{2a}, \qquad \max \gamma_{12}^i \le \gamma_{12a}$$
$$i = 1, \ldots, n$$

where ε_{1a} is allowable strain in the fiber direction; ε_{2a} is allowable strain in the transverse direction; γ_{12a} is allowable shear strain; $\max \varepsilon_1^i$, $\max \varepsilon_2^i$, and $\max \gamma_{12}^i$ are maximum values of these strains within the panel i; the buckling load constraint $\lambda_b \ge 1.0$, where λ_b is the lowest buckling load factor obtained as a solution of an eigenvalue problem; and the percentage of plies of each orientation is $\ge 10\%$.

A finite element analysis (FEA) software ANSYS [28] is used for calculating strains and the buckling load factor λ_b. As it also incorporates a gradient-based optimization method, it is used to solve the top-level optimization problem. If gradients of the response functions are evaluated by the finite differences (as in ANSYS), the total number of calls for the FE analysis (including an eigenvalue analysis) is growing approximately linearly with the growing number of design variables. If an FE sensitivity analysis is used (e.g., as in OptiStruct [27]), the overall computational efficiency can be greatly improved. In our research, ANSYS Parametric Design Language (APDL) was used to define the FE stiffness matrix according to Eq. (4). At the local (bottom) level, Altair's HyperShuffle [26,29] is used for arranging a given number of plies of each orientation (obtained in the top-level optimization) into a stacking sequence that satisfies the composite design rules. Ply shuffling in the stack is performed in such a way that the stack composition remains as uniform as possible while satisfying the composite design rules. Ply shuffling does not alter the strain values, and the buckling load of the shuffled stack also remains quite similar to that of the homogeneous composite material handled in the top-level optimization, although this cannot be always guaranteed. The advantage of this method is that it avoids a stacking-sequence optimization at the local (bottom) level by performing a quicker postprocessing function of ply shuffling. The fact that ply shuffling can lead to a (slight) violation of the buckling constraint, particularly when shuffling is performed many times in the blending procedure as described below, can be considered a disadvantage.

B. Lamination-Parameter-Based Method

Lamination parameters were first introduced in [7]. It is known that the stiffness matrices **A** and **D** are governed by 12 lamination parameters and five material parameters. For orthotropic symmetric and balanced laminates, the number of independent lamination parameters can be reduced to eight. The elements of the membrane stiffness matrix **A** and the bending stiffness matrix **D** can be expressed as

$$\begin{bmatrix} A_{11} \\ A_{22} \\ A_{12} \\ A_{66} \\ A_{16} \\ A_{26} \end{bmatrix} = h \begin{bmatrix} 1 & \xi_1^A & \xi_3^A & 0 & 0 \\ 1 & -\xi_1^A & \xi_3^A & 0 & 0 \\ 0 & 0 & -\xi_3^A & 1 & 0 \\ 0 & 0 & -\xi_3^A & 0 & 1 \\ 0 & \xi_2^A/2 & \xi_4^A & 0 & 0 \\ 0 & \xi_2^A/2 & -\xi_4^A & 0 & 0 \end{bmatrix} \begin{bmatrix} U_1 \\ U_2 \\ U_3 \\ U_4 \\ U_5 \end{bmatrix}$$

$$\begin{bmatrix} D_{11} \\ D_{22} \\ D_{12} \\ D_{66} \\ D_{16} \\ D_{26} \end{bmatrix} = \left(\frac{h^3}{12}\right) \begin{bmatrix} 1 & \xi_1^D & \xi_3^D & 0 & 0 \\ 1 & -\xi_1^D & \xi_3^D & 0 & 0 \\ 0 & 0 & -\xi_3^D & 1 & 0 \\ 0 & 0 & -\xi_3^D & 0 & 1 \\ 0 & \xi_2^D/2 & \xi_4^D & 0 & 0 \\ 0 & \xi_2^D/2 & -\xi_4^D & 0 & 0 \end{bmatrix} \begin{bmatrix} U_1 \\ U_2 \\ U_3 \\ U_4 \\ U_5 \end{bmatrix} \tag{5}$$

where the lamination parameters are

$$\xi^A_{[1,2,3,4]} = \frac{1}{h}\int_{-h_i/2}^{h_i/2} [\cos 2\theta, \sin 2\theta, \cos 4\theta, \sin 4\theta]\, \mathrm{d}z \quad \text{and}$$

$$\xi^D_{[1,2,3,4]} = \frac{12}{h^3}\int_{-h_i/2}^{h_i/2} [\cos 2\theta, \sin 2\theta, \cos 4\theta, \sin 4\theta] z^2\, \mathrm{d}z$$

This suggests that the use of lamination parameters as design variables in the composite optimization can be very beneficial. It is known (see [1,12]) that the relationships between the out-of-plane lamination parameters can be expressed as

$$2(1+\xi_3^D)(\xi_2^D)^2 - 4\xi_1^D\xi_2^D\xi_4^D + (\xi_4^D)^2 \le (\xi_3^D - 2(\xi_1^D)^2 + 1)(1-\xi_3^D)$$

$$(\xi_1^D)^2 + (\xi_2^D)^2 \le 1 \qquad 2(\xi_1^D)^2 - 1 \le \xi_3^D \le 1 \tag{6}$$

For the majority of astronautical structures, symmetric and balanced laminates with ply orientations of 0, 90, 45, and −45 deg are used. Thus, $\xi_4^D = 0$ and the first relationship in (6) can be rewritten as

$$(\xi_2^D)^2 \le \frac{(\xi_3^D - 2(\xi_1^D)^2 + 1)(1-\xi_3^D)}{2(1+\xi_3^D)} \tag{7}$$

In addition, a group of relationships between the in-plane and out-of-plane lamination parameters for the symmetric laminates are available (see [12–15,30,31]). These expressions can be formulated as additional constraints for the top-level optimization problem:

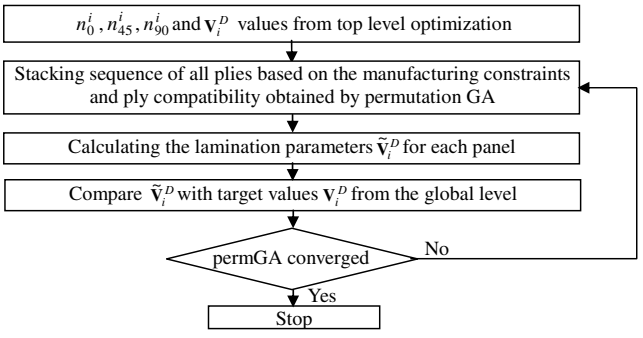

Fig. 1 Flowchart of the panel stacking-sequence optimization process.

$$\begin{aligned}
&(\xi_i^A - 1)^4 - 4(\xi_i^D - 1)(\xi_i^A - 1) \le 0 \qquad i = 1,2,3\\
&(\xi_i^A + 1)^4 - 4(\xi_i^D + 1)(\xi_i^A + 1) \le 0 \qquad i = 1,2,3\\
&(2\xi_1^A - \xi_3^A - 1)^4 - 16(2\xi_1^D - \xi_3^D - 1)(2\xi_1^A - \xi_3^A - 1) \le 0\\
&(2\xi_1^A + \xi_3^A + 1)^4 - 16(2\xi_1^D + \xi_3^D + 1)(2\xi_1^A + \xi_3^A + 1) \le 0\\
&(2\xi_1^A - \xi_3^A + 3)^4 - 16(2\xi_1^D - \xi_3^D + 3)(2\xi_1^A - \xi_3^A + 3) \le 0\\
&(2\xi_1^A + \xi_3^A - 3)^4 - 16(2\xi_1^D + \xi_3^D - 3)(2\xi_1^A + \xi_3^A - 3) \le 0\\
&(2\xi_2^A - \xi_3^A + 1)^4 - 16(2\xi_2^D - \xi_3^D + 1)(2\xi_2^A - \xi_3^A + 1) \le 0\\
&(2\xi_2^A + \xi_3^A - 1)^4 - 16(2\xi_2^D + \xi_3^D - 1)(2\xi_2^A + \xi_3^A - 1) \le 0\\
&(2\xi_2^A - \xi_3^A - 3)^4 - 16(2\xi_2^D - \xi_3^D - 3)(2\xi_2^A - \xi_3^A - 3) \le 0\\
&(2\xi_2^A + \xi_3^A + 3)^4 - 16(2\xi_2^D + \xi_3^D + 3)(2\xi_2^A + \xi_3^A + 3) \le 0\\
&(\xi_1^A - \xi_2^A - 1)^4 - 4(\xi_1^D - \xi_2^D - 1)(\xi_1^A - \xi_2^A - 1) \le 0\\
&(\xi_1^A + \xi_2^A + 1)^4 - 4(\xi_1^D + \xi_2^D + 1)(\xi_1^A + \xi_2^A + 1) \le 0\\
&(\xi_1^A - \xi_2^A + 1)^4 - 4(\xi_1^D - \xi_2^D + 1)(\xi_1^A - \xi_2^A + 1) \le 0\\
&(\xi_1^A + \xi_2^A - 1)^4 - 4(\xi_1^D + \xi_2^D - 1)(\xi_1^A + \xi_2^A - 1) \le 0
\end{aligned} \tag{8}$$

In this paper, the lamination parameters are defined as

$$\begin{aligned}
\xi^A_{0,i} &= \left(\frac{1}{h_i}\right)\int_{-h_i/2}^{h_i/2} 1\, \mathrm{d}z = 2(n_0^i + n_{90}^i + 2n_{45}^i) = 1\\
\xi^A_{1,i} &= \left(\frac{1}{h_i}\right)\int_{-h_i/2}^{h_i/2} \cos 2\theta\, \mathrm{d}z = 2(n_0^i - n_{90}^i) = \frac{n_0^i - n_{90}^i}{n_0^i + n_{90}^i + 2n_{45}^i}\\
\xi^A_{2,i} &= \left(\frac{1}{h_i}\right)\int_{-h_i/2}^{h_i/2} \sin 2\theta\, \mathrm{d}z = 0\\
\xi^A_{3,i} &= \left(\frac{1}{h_i}\right)\int_{-h_i/2}^{h_i/2} \cos 4\theta\, \mathrm{d}z = 2(n_0^i + n_{90}^i - 2n_{45}^i)\\
&= \frac{n_0^i + n_{90}^i - 2n_{45}^i}{n_0^i + n_{90}^i + 2n_{45}^i}\\
\xi^A_{4,i} &= \left(\frac{1}{h_i}\right)\int_{-h_i/2}^{h_i/2} \sin 4\theta\, \mathrm{d}z = 0\\
V^D_{[1,2,3,4],i} &= 1 + \frac{2}{3}\xi^D_{[1,2,3,4]} = 1\\
&\quad + \left(\frac{2}{h_i}\right)^3 \int_{-h_i/2}^{h_i/2} [\cos 2\theta, \sin 2\theta, \cos 4\theta, \sin 4\theta] z^2\, \mathrm{d}z
\end{aligned} \tag{9}$$

where A and D indicate membrane and bending effects, i is the panel number, n_0^i is half the number of 0 deg plies in the total stack of the ith panel, n_{45}^i is half the number of pairs of ±45 deg plies in the total stack of the ith panel, n_{90}^i is half the number of 90 deg plies in the total stack of the ith panel, h_i is the total thickness of the panel i, and θ is the ply angle.

In the formulas above, the values $V^D_{0,i} = 1 + 2/3$ and $V^D_{4,i} = 1$ can be immediately evaluated, and the following condition holds: $V^D_{[1,2,3],i} \ge 0$.

In this approach, the top-level optimization problem formulation is as follows:

$$\text{Minimize} \sum_{i=1}^{n} (n_0^i + n_{45}^i + n_{90}^i) A_i t$$

where t is the ply thickness, n is the total number of panels, and A_i is the area of panel i.

The design variables are the numbers of plies of each orientation n_0^i, n_{45}^i, n_{90}^i and the out-of-plane lamination parameters V_j^i ($i = 1, \ldots, n$, $j = 1, 2, 3$). The strain constraints are

$$\max \varepsilon_1^i \le \varepsilon_{1a}, \qquad \max \varepsilon_2^i \le \varepsilon_{2a}, \qquad \max \gamma_{12}^i \le \gamma_{12a}$$
$$i = 1, \ldots, n$$

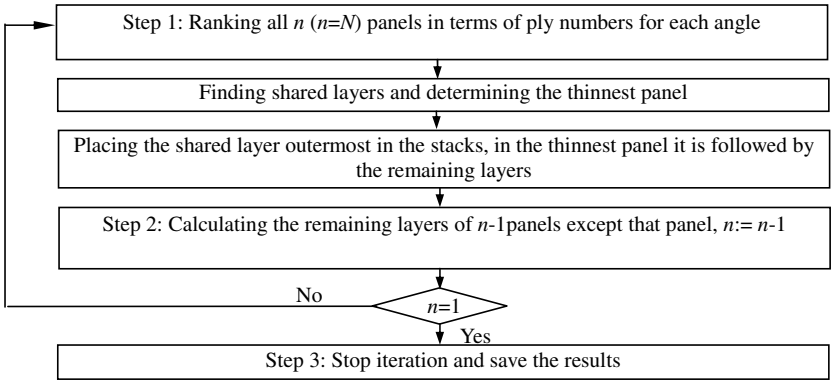

Fig. 2 Flowchart for the shared-layer blending scheme.

where ε_{1a} is allowable strain in the fiber direction; ε_{2a} is allowable strain in the transverse direction; γ_{12a} is allowable shear strain; $\max \varepsilon_1^i$, $\max \varepsilon_2^i$, and and $\max \gamma_{12}^i$ are maximum values of these strains within the panel i; the buckling load constraint $\lambda_b \geq 1.0$, where λ_b is the lowest buckling load factor obtained as a solution of an eigenvalue problem; and the percentage of plies of each orientation is $\geq 10\%$ feasibility of lamination parameters defined by Eqs. (6–8).

An FEA software ANSYS [28] is used for calculating strains and the buckling load factor λ_b. APDL was used to define the FE stiffness matrix according to Eq. (5).

To solve this optimization problem, a gradient-based optimization method available in ANSYS was used for all examples given in Sec. VII. As convexity of the top-level optimization problem is not proven, the uniqueness of the solution cannot be guaranteed. For example, in Sec. VII, from a limited number of trials with different starting values of design variables, we observed convergence to almost the same solution in the numbers of plies of each orientation and the lamination parameters $\mathbf{V}_1^D$ and $\mathbf{V}_2^D$, but a larger variation in the lamination parameter $\mathbf{V}_3^D$.

In the local level, a stacking-sequence optimization is performed by matching the lamination parameters $\mathbf{V}_i^D$ that came from the top-level optimization with the lamination parameters $\tilde{\mathbf{V}}_i^D$ computed in the local level optimization in a least squares sense subject to satisfaction of the composite design rules and manufacturing requirements. A permGA is used for the local level optimization runs carried out iteratively in order to ensure the ply compatibility of adjacent panels, as presented in Sec. IV. A schematic of the optimization process at this level is shown in Fig. 1. The advantage of this approach is that there is no need to check whether the strain or buckling constraints have been violated as long as the lamination parameters obtained after the local level optimization match the given lamination parameter values that came from the top-level optimization. In the ply compatibility optimization process it is also required to keep the values of lamination parameters in all the panels of the whole structure matching the corresponding values that came from the top-level optimization.

III. Composite Design Rules

According to aircraft industry manufacturing requirements [24,32], the laminate layup design rules applied to each panel are as follows:

1) The laminate is balanced, i.e., the number of 45, and −45 deg plies is the same in each of the components.

2) Because of the damage-tolerance requirements, the outer plies for the skin should always contain at least one set of ±45 deg plies.

3) The number of plies ($N_{\max}$) in any one direction placed sequentially in the stack is limited to four.

4) A 90 deg change of angle between two adjacent plies is to be avoided, if possible.

IV. Shared-Layer Blending

In aerospace engineering, a typical wing is a multipanel tailored composite structure. To improve structural integrity and avoid stress concentration between two adjacent panels, ply blending should be ensured. Although such requirements have been considered in [17–24], a problem of optimization of multipanel aircraft structures with a comprehensive consideration of buckling, strain, manufacturing constraints as well as general composite design rules including ply blending still remains to be addressed to the satisfaction of aircraft industry.

In this section the shared-layer blending process is applied to satisfy the global blending requirement as well as the general layup design rules. Three illustrative examples are given to demonstrate this process.

First, ranking of all panels in terms of the numbers of plies of each angle is performed. Then for each ply angle, out of all panels the minimum number of plies is selected. This set of three ply numbers defines the first set of shared layers among all panels. The thinnest panel that includes the first shared layers is identified. The first shared layers will be placed outermost in the stacks for all panels. The remaining layers in the thinnest panel are placed after the first shared layers. Next, after this first stage, for the remaining layers of all the panels, except the thinnest panel, the same procedure is applied as at the first stage. This is repeated until the last panel is considered. Finally, for the adjacent panels, the local blending between them is performed for the remaining layers in the adjacent panels. The scheme for the local blending consideration is given in example 2. Thus, the plies for all the panels will become inwardly blended (outer blending), when the outer layers of all the panels are continuous. If the shared layers are placed at the position next to the midplane instead of the outermost position, the inner blending (outwardly blended) composite will be created. In this paper, the outer blending procedure is adopted due to the damage-tolerance requirements resulting in ±45 deg plies placed on the outside of the stack.

A flowchart of the shared-layer blending approach is shown in Fig. 2.

Example 1: In the first example three panels are linked together with the numbers of plies of each orientation (as coming from the top-level optimization) given in Table 1.

Using this approach, the first set of shared layers in this example will be $n_0/n_{45}/n_{90} = 29/6/7$ (that is $29 + 2 \times 6 + 7 = 48$ plies) for all three panels, and panel 3 is selected as the first (thinnest) panel. The second shared set will be $n_0/n_{45}/n_{90} = 6/8/0$ (22 plies) for panels 1 and 2 only. Now the remaining layers in the three-panel structure will be $n_0/n_{45}/n_{90} = 5/3/0$ (11 plies) for panel 1, $n_0/n_{45}/n_{90} = 0/0/2$ (two plies) for panel 2, and $n_0/n_{45}/n_{90} = 0/0/5$ (five plies) for panel 3. In this example, because no shared

Table 1 Numbers of plies of each orientation for a three-panel laminated structure

Panel no.	Number of plies $n_0/n_{45}/n_{90}$
1	40/17/7
2	35/14/9
3	29/6/12

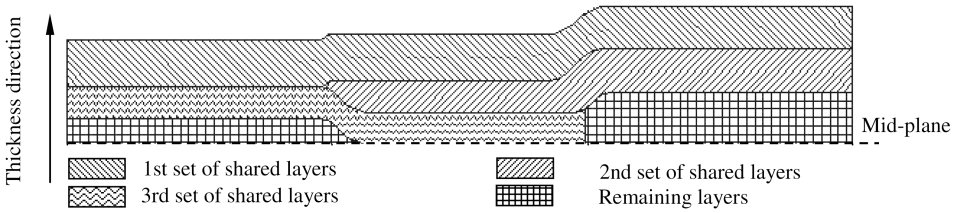

Fig. 3 Illustration of shared-layer blending concept for the three-panel linked structure.

layers are available between panels 1 and 2, the local shared set will be $n_0/n_{45}/n_{90} = 0/0/2$ (two plies) for the remaining layers in panels 2 and 3. Note that for a case of a panel that is adjacent to several panels, the scheme for consideration of local blending of remaining layers among these panels will be shown in example 2 below. Thus, the remaining layers in panel 1 after the shared-layer blending procedure will be $n_0/n_{45}/n_{90} = 5/3/0$ (11 plies), no remaining layers left in panel 2, and $0/0/3$ (three plies) in panel 3. The blending schematic is shown in Fig. 3.

Two issues arise from the results in example 1 that need to be addressed in the blending scheme. The first one is that the group of remaining layers in panel 3 consists only of five 90 deg plies that violate the ply composition rule. The second issue is that the total number of plies in the second set of shared layers truncated between the adjacent panels 2 and 3 can be considered too large.

For the first issue, having five 90 deg plies as remaining layers in panel 3 means that too many plies were selected for the first set of shared layers. A slightly larger number of plies including at least one or ± 45 deg ply have to be included into the set of remaining layers for panel 3. Therefore, having more than four plies of the same orientation together can be avoided in panel 3 by reserving some layers from the first set of shared layers. For example, one ply of 0 fiber orientation can be extracted from the first set of shared layers and inserted into the remaining layers for panel 3 to separate the group of five 90 deg plies. Thus, the first set of shared layers will be $n_0/n_{45}/n_{90} = 28/6/7$ (47 plies) and the second set of shared layers will be $n_0/n_{45}/n_{90} = 7/8/0$ (23 plies). The local shared set will be still $n_0/n_{45}/n_{90} = 0/0/2$ (two plies) and the remaining layers for panel 3 will be $n_0/n_{45}/n_{90} = 1/0/3$ (four plies). For the second issue, let us assume that the number of truncated plies between panels 2 and 3 is too large. This means that too many plies are selected as the second set of shared layers in the above blending procedure. Thus, the number of plies used as the second set of shared layers has to be readjusted to satisfy the requirement. Generally, for practical stack compositions that satisfy realistic constraints on ply orientation percentages, a solution for a stacking-sequence repair can always be found: if a problem happens at a certain stage, the algorithm steps back and plies are removed from the previous set of shared layers in the above blending scheme. This is repeated iteratively until the obtained stacking sequence satisfies all the design rules and constraints.

Example 2: The neighbor panel selection scheme for local blending will be explained in this example. A six-panel structure with the numbers of plies of each orientation is shown in Fig. 4. In this example, the ranking order of the thicknesses for all six panels is from

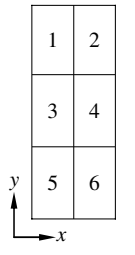

a)

Panel	Number of plies
1	15/12/4
2	16/11/3
3	17/6/5
4	14/5/2
5	15/2/5
6	13/2/3

b)

Fig. 4 Illustration of local blending concept for six-panel laminated structure: a) geometry of the structure and b) numbers of plies of each orientation.

panel 6 (thinnest) to panel 1 (thickest). Using the blending scheme above, the first set of shared layers in this example will be $n_0/n_{45}/n_{90} = 13/2/2$ for all six panels and panel 6 is selected as the first (thinnest) panel. Next, the second set of shared layer is $n_0/n_{45}/n_{90} = 1/0/0$ for all the other five panels (from panel 1 to panel 5). Then the third set of shared layers is $n_0/n_{45}/n_{90} = 0/3/0$ for all the other fours panels (from panel 1 to panel 4). The fourth set of shared layers is $n_0/n_{45}/n_{90} = 1/1/1$ for the remaining three panels (from panel 1 to panel 3). The last (fifth) set of shared layers is $n_0/n_{45}/n_{90} = 0/5/0$ for panels 1 and 2. Thus, the remaining layers can be listed as panel 1: $n_0/n_{45}/n_{90} = 0/1/1$; panel 2: $n_0/n_{45}/n_{90} = 1/0/0$; panel 3: $n_0/n_{45}/n_{90} = 2/0/2$; panel 4: $n_0/n_{45}/n_{90} = 0/0/0$; panel 5: $n_0/n_{45}/n_{90} = 1/0/3$; and panel 6: $n_0/n_{45}/n_{90} = 0/0/1$. The order of considering the local blending for adjacent panels such as the pair of panels 5 and 6 and the pair of panels 5 and 3 will be determined by the corresponding thickness jump. The latter means the difference of the thicknesses of the two adjacent panels that is known from the top-level optimization. Since the thickness jump in the x direction is smaller than that in the y direction in this example, the local blending between the panels 5 and 6 will be considered before the blending between panels 3 and 5. When several adjacent panels follow the same direction, for example, the adjacent panels 1 and 3 and the adjacent panels 3 and 5 follow the y direction, the order of local blending will follow the direction which reflects the distributions of the panel thickness: from the thinnest to the thickest. This means that the direction will be from panel 5 to panel 1, through panel 3. Thus, the local blending between panels 3 and 5 will be considered before the blending between panels 1 and 3.

V. Calculation of Lamination Parameters in the Blending Scheme

In the optimization using the lamination-parameter-based method, lamination parameters are calculated at the local level to match the target values from the top level. The lamination parameters are calculated simultaneously with the blending scheme described in Sec. IV. Once the first set of shared layers is determined by the blending scheme, the stacking sequence for the first set of shared layers will be obtained by a permutation GA to match the lamination parameters from the top level in the thinnest panel. Following that the values of lamination parameters corresponding to the first set of shared layers in each of the remaining panels are calculated. Generally, these values will be different in different panels because, following the outer blending scheme, the distance of the shared layers from the midplane varies from panel to panel. Next, the same blending scheme of determining the second set of shared layers is applied. The stacking sequence of the second set of shared layers will be determined to match the difference between the lamination parameters from the top level and the values already calculated for the first set of shared layers in the next thinnest panel (because the first thinnest panel has already been dealt with). This is repeated until the last set of shared layers is considered. Then lamination parameters contributed from the sets of shared layers are summed up for each panel. Finally, the stacking sequence of remaining layers in each panel will be determined to minimize the difference between the lamination parameters from the top level and those summed up in the blending scheme. An example below will demonstrate this procedure.

Example 3: In this example three panels are sequentially linked with the numbers of plies of each orientation and lamination

Table 2 Numbers of plies of each orientation and lamination parameters for a three-panel laminated structure

	Panel 1	Panel 2	Panel 3
Number of plies $(n_0/n_{45}/n_{90})$	15/4/3	12/3/6	10/3/5
V_1^D	1.1203	1.1400	1.2034
V_2^D	1.0092	1.0056	1.0078
V_3^D	1.2032	1.2932	1.0728

parameters related to the bending stiffness matrix (as coming from the top-level optimization) given in Table 2.

The first set of shared layers in this example will be $n_0/n_{45}/n_{90} = 10/3/3$ for all three panels, and panel 3 is also selected as the first (thinnest) panel. The stacking sequence of the first set of shared layers will be obtained by the permutation GA to match the lamination parameters from the top level ($\mathbf{V}_i^D = [V_{1,i}^D, V_{2,i}^D, V_{3,i}^D]$) for panel 3. The values $\tilde{\mathbf{V}}_{i,(j)}^D$ will represent the contribution of the lamination parameters calculated for the jth set of shared layers in the ith panel. In this example, the lamination parameters calculated for the first set of shared layers in panel 3 are $\tilde{\mathbf{V}}_{3,(1)}^D = [1.1920, 1.0068, 1.0718]$. At the same time, the contribution of lamination parameters from the stacking sequence of the first set of shared layers to panels 2 and 1 can be calculated as $\tilde{\mathbf{V}}_{2,(1)}^D = [1.1632, 1.0038, 1.2808]$ and $\tilde{\mathbf{V}}_{1,(1)}^D = [1.1430, 1.0068, 1.1878]$, respectively. After the first blending stage, the differences between the lamination parameters from the top level and the values calculated from the first set of shared layers in panels 2 and 1 are $\mathbf{V}_2^D - \tilde{\mathbf{V}}_{2,(1)}^D = [-0.0232, 0.0018, 0.0124]$ and $\mathbf{V}_1^D - \tilde{\mathbf{V}}_{1,(1)}^D = [-0.0227, 0.0024, 0.0154]$, respectively. Then the stacking sequence of the second set of shared layers ($n_0/n_{45}/n_{90} = 2/0/0$) will be determined to target the difference in panel 2 (although the stacking sequence is trivial in this case). The contributions of lamination parameters calculated from the stacking sequence of the second set of shared layers to panels 2 and 1 are $\tilde{\mathbf{V}}_{2,(2)}^D = [-0.0032, 0.0010, 0.0114]$ and $\tilde{\mathbf{V}}_{1,(2)}^D = [-0.049, 0.0012, 0.0134]$, respectively. The remaining layers after the global blending scheme are for panel 1: $n_0/n_{45}/n_{90} = 3/1/0$; for panel 2: $n_0/n_{45}/n_{90} = 0/0/3$; for panel 3: $n_0/n_{45}/n_{90} = 0/0/2$. Now the local blending will be applied to determine the third set of shared layers between panels 3 and 2 that is $n_0/n_{45}/n_{90} = 0/0/2$. The stacking sequence of the third set of shared layers will be determined to target the difference in panel 3. The difference between the lamination parameters from the top level and the values calculated from the first set of shared layers is $\mathbf{V}_3^D - \tilde{\mathbf{V}}_{3,(1)}^D = [0.0114, 0.0010, 0.0010]$. The contributions of the lamination parameters from the stacking sequence of the third set of shared layers to panels 2 and 3 can be calculated as $\tilde{\mathbf{V}}_{3,(3)}^D = [0.0010, 0.0002, 0.0006]$ and $\tilde{\mathbf{V}}_{2,(3)}^D = [0.0012, 0.0005, 0.0008]$, respectively. Finally, the remaining layers after the blending are for panel 1: $n_0/n_{45}/n_{90} = 3/1/0$; for panel 2: $n_0/n_{45}/n_{90} = 0/0/1$ and no remaining layers are left for panel 3. The summation of the lamination parameters for each panel will produce for panel 1: $\tilde{\mathbf{V}}_{1,(1)}^D + \tilde{\mathbf{V}}_{1,(2)}^D = [1.0940, 1.0080, 1.2012]$; for panel 2: $\tilde{\mathbf{V}}_{2,(1)}^D + \tilde{\mathbf{V}}_{2,(2)}^D + \tilde{\mathbf{V}}_{2,(3)}^D = [1.1612, 1.0053, 1.2930]$ and for panel 3: $\tilde{\mathbf{V}}_{3,(1)}^D + \tilde{\mathbf{V}}_{3,(3)}^D = [1.1930, 1.0070, 1.0724]$. For panel 3, there are no remaining layers left and the calculated lamination parameters are $\tilde{\mathbf{V}}_3^D = [1.1930, 1.0070, 1.0724]$. The stacking sequences of the remaining layers in panels 2 and 1 will be obtained to target the difference between the lamination parameters $\mathbf{V}_i^D$ from top level and those summed up in the blending scheme, respectively.

VI. Permutation GA

In the lamination-parameter-based method, the number of plies of each orientation and the lamination parameters related to the out-of-plane stiffness matrix are obtained from the top-level optimization. The local level optimization aims at preserving the given values of the out-of-plane lamination parameters while shuffling the given number of plies to satisfy the layup rules and blending requirements. A permutation GA is an ideal tool for such a composite laminate optimization problem. Each string in the coding represents a unique stacking sequence. An example of using the genetic operators with a permutation encoding is given below.

1) Mutation-two numbers are selected and exchanged, e.g., third and fifth:

$$[1 \quad 2 \quad 3 \quad 4 \quad 5] \Rightarrow [1 \quad 2 \quad 5 \quad 4 \quad 3]$$

2) Crossover can be done in a variety of ways, such as simple crossover, cycle crossover, inversion, and swap adjacent cells. The swap adjacent cells method implemented in this work is illustrated below:

$$[1 \quad 2 \quad 3 \quad 4 \quad 5] \Rightarrow [1 \quad 3 \quad 2 \quad 4 \quad 5]$$

To reflect the layup rules of composite laminate design and manufacturing requirements, substrings that represent stacking sequences of layers such as $45/0/-45, 45/90/-45, 45/0_2/-45$ and $45/90_2/-45$ are implemented in the permutation GA coding in order to improve the stacking-sequence design of composite laminates.

It should be noted that, as no calls for an FE analysis are made in the local level optimization, the fitness function evaluation involves only calculation of lamination parameters by simple formulas. Hence, it is a quick optimization step that takes much less time (typically, a few minutes on a low-specification PC) than the FE-based top-level optimization. The following settings of the permGA were used in the examples in Sec. VII: a population size of 600, 500 generations, elite as 5% of the population, tournament selection, and a swap adjacent cells crossover.

VII. Wing Box Example

The benchmark wing box model [5] used to illustrate the methods discussed in previous sections is shown in Figs. 5 and 6. For modeling top and bottom skins, ribs and spars in ANSYS, four-node quadrilateral finite elements (Shell181) were used. As in [5], spars and ribs are assumed to be symmetric and balanced laminates with the fixed stacking sequence $[\pm 45_{11}]_s$. All the laminates are made of graphite-epoxy T300/5208 whose material properties are shown in Table 3. It should be noted that in this example the allowable strains have been made artificially high in order to force the buckling constraint to be critical for the top skin panels. Four point loads F_1,

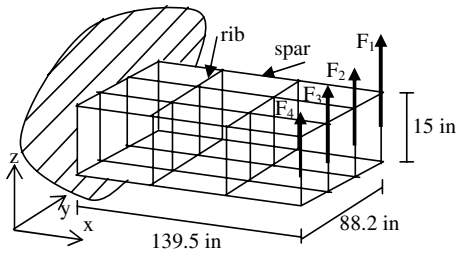

Fig. 5 Geometry of the wing box.

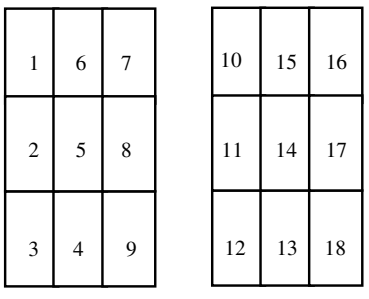

Fig. 6 Bottom and top skin configurations.

Table 3 Material properties for graphite-epoxy T300/N5208

Material properties	Values
Young's modulus in the fiber direction 1, E_1	127.56 GPa
Young's modulus in the transverse direction 2, E_2	13.03 GPa
Shear modulus G_{12}	6.41 GPa
Poisson's ratio ν_{12}	0.3
Material density ρ	1577.76 kg/m^3
Ply thickness t	0.127 mm
Allowable strain in the fiber direction, ε_{1a}	0.08
Allowable strain in the transverse direction, ε_{2a}	0.029
Allowable shear strain, γ_{12a}	0.015
Safety factor	1.5

F_2, F_3, and F_4 of magnitudes 380,176.16, 187,888.44, 187,888.44, and 90,009.77 N are applied at the central line of the rib at the free end to avoid the local stress effects on the top skin. These loads induce both upward bending and twisting of the wing box. Because of the aircraft industry manufacturing requirements, 0 or 90 deg plies are required to be inserted into pairs of ±45 plies to avoid 90 deg change between two adjacent plies. Thus, the bending–twisting coupling terms D_{16} and D_{26} are nonzero from the contributions of offaxis layers and the distance of the positive and negative angle plies from the laminate center plane. In this work, the number of 45 deg plies in the top skin and the number of 0 and 90 deg plies in the bottom skin are rounded up to achieve the discrete optimal design.

A. Problem with Two Designable Substructures

If the layup of all panels in the top skin is the same and all the bottom skin panels are also the same, the total number of design variables for the wing box is six (n_0^t, $n_{\pm 45}^t$, n_{90}^t, n_0^b, $n_{\pm 45}^b$, and n_{90}^b, where superscript t means the top skin and b stands for the bottom skin) in the smeared-stiffness-based method. In the lamination-parameter-based method six additional nondimensional design variables V_1^{Dt}, V_2^{Dt}, V_3^{Dt}, V_1^{Db}, V_2^{Db}, and V_3^{Db} related to the bending stiffness matrix are needed. The results for the objective function and the violation of constraints at the top level are shown in Table 4 for the smeared-stiffness-based method and Table 5 for the lamination-parameter-based method. Considering the smeared-stiffness-based method first, for the continuous optimal design the buckling constraint is active for panel 16. The top skin is much heavier than the bottom skin, due to the buckling constraints. In contrast with the results from [5], the objective function is reduced to 2.082×10^7 mm^3 as compared to 2.329×10^7 mm^3. In the local level optimization, shuffling all the layers from the top-level optimization is performed according to the layup rules, and the result is shown in Table 6. For the optimal design with the lamination-parameter-based method, a lighter structure (2.015×10^7 mm^3) has been obtained than that with smeared-stiffness-based method (2.082×10^7 mm^3). In the local level optimization, given the lamination parameters from the top level, a permutation GA is used to obtain the stacking sequence for the top and bottom skins, as presented in Tables 7 and 8. The buckling mode for the obtained structure corresponds to the top skin buckling. The values of lamination parameters $\tilde{V}_1^D$, $\tilde{V}_2^D$, and $\tilde{V}_3^D$ produced by the local level optimization (Table 7) compare well to the target values V_1^D, V_2^D, and V_3^D (Table 5) for the top skin that has 76 plies in half-stack. The bottom skin is much thinner (14 plies in the half-stack); hence, the match of lamination parameters is considerably less accurate. The out-of-plane lamination parameters for the bottom skin do not have a significant effect on the buckling of the top skin, because the bottom skin is mainly subjected to shear and tensile loads.

B. Problem with Six Designable Substructures

If the top and bottom skins are divided into three parts (root, intermediate, and tip part), the results are listed in Tables 9–13.

Table 4 Optimal designs with six variables for the smeared-stiffness-based method

	n_0	n_{45}	n_{90}	n_0	n_{45}	n_{90}	
	Continuous			Rounded			Active constraints
Top skin panels	40.95	10.45	16.39	41	11	16	Panel 16 (buckling)
Bottom skin panels	5.67	1.48	5.17	6	1	6	——
Buckling load factor	0.990	——	——	1.022	——	——	——
Total number of plies	184.11	——	——	186	——	——	——
Total number of plies [5]	208.76	——	——	208	——	——	——
Total volume, mm^3	2.061e7	——	——	2.082e7	——	——	——
Total volume [5], mm^3	2.337e7	——	——	2.329e7	——	——	——

Table 5 Optimal designs with 12 variables for the lamination-parameter-based method

	n_0	n_{45}	n_{90}	n_0	n_{45}	n_{90}	
	Continuous			Rounded			Buckling load factor
Top skin panels	34.492	7.445	26.139	34	8	26	1.0009
Bottom skin panels	8.163	1.480	2.181	9	1	3	1.0183
Lamination parameters	V_1^D	V_2^D	V_3^D	——	——	——	——
Top skin panels	0.9434	1.0065	1.2108	——	——	——	——
Bottom skin panels	0.8944	1.0435	0.9710	——	——	——	——
Total number of plies	177.65	——	——	180	——	——	——
Results from [5]	208.76	——	——	208	——	——	——
Total volume, mm^3	1.989e7	——	——	2.015e7	——	——	——
Total volume [5], mm^3	2.337e7	——	——	2.329e7	——	——	——

Table 6 Stacking sequence of the top and bottom skin panels for the optimal design with six variables

Panel no.	Stacking sequence
Top skin panel	$[(\pm 45)_2/(0_4/90/45/0/-45)_3/(0_4/90/45/90/-45)_5/0_4/90/45/0/-45/90_2/0]_s$
Bottom skin panel	$[\pm 45/0_3/90_3/0_2/90_3/0]_s$
Buckling load factor	1.020

Table 7 Lamination parameters of the panels with 12 variables

Panel	$\tilde{V}_1^D$	$\tilde{V}_2^D$	$\tilde{V}_3^D$
Top skin panels[a]	0.9434	1.0080	1.2107
Bottom skin panels	1.0131	1.0190	1.1730

[a]Buckling load factor is 1.0178 (panel 16).

Results in Tables 9 and 10 correspond to the smeared-stiffness-based method. The total material volume is reduced from 2.082×10^7 mm^3 (as in the case of two designable substructures above) to 1.710×10^7 mm^3. For the optimal designs obtained with the lamination-parameter-based method, the total material volume is reduced from 2.015×10^7 mm^3 to 1.726×10^7 mm^3. The first and the second buckling modes are shown in Figs. 7 and 8. It should be noted that shear buckling occurred in the bottom skin (buckling load reduction by 4%), as shown in Tables 12 and 13. This is due to the application of a blending procedure to a part of the structure (bottom skin) that has a relatively few plies, in which case blending caused a poor match between the target and obtained values of lamination parameters. This can be repaired by adding some layers manually. The second buckling mode corresponds to the top skin; the magnitude of the load factor is close to the value from the top-level optimization. This is guaranteed by arriving at a good match with the lamination parameters from top-level optimization when a local optimization is performed. By comparison of the results from Tables 9 and 11, a slightly larger number of plies (456.68) are obtained for a continuous optimal design with the lamination-parameter-based method than those (448.82) with the smeared-stiffness-based method as the buckling load factor is increased from 0.9960 to 1.0039. The values of lamination parameters produced by the local level optimization in Tables 12 and 13 can be compared to the target values in Table 11. Summarizing, due to the limited number of plies in the bottom panel, it was difficult to shuffle the plies to match the lamination parameters from the top level while satisfying ply continuity in the bottom skin. For the top skin (which has a much greater number of plies), the lamination parameters are quite close to those from the top-level optimization, and the outer blending with the layup rules requirements did not cause any problems.

C. Problem with Nine Designable Substructures

Because of the limitation on the number of design variables in ANSYS, all panels in the top skin only are considered designable in the top-level optimization and the configuration of panels in the bottom skin is fixed and is the same as the discrete optimal results for the case of six designable substructures above. For the smeared-stiffness-based method, it can be seen that the buckling is prevented in the discrete optimal design and the number of plies was increased from 1171.9 to 1192 (Table 14). Because of the blending requirements in the local optimization, the first buckling mode happens in the bottom skin and the second in the top skin. This can be repaired by a manual adjustment. For the lamination-parameter-based method, a slightly greater number of plies (1177.32) are obtained for the continuous optimal design than those (1171.9) for the smeared-stiffness-based method. The buckling load factor is increased from 0.9967 to 1.0014 (see Tables 14 and 16). With the objective to target the lamination parameters from the top level, the plies are shuffled while satisfying the blending considerations. Since

Table 8 Stacking sequence of the panels with 12 variables

Panel	Stacking sequence
Top skin panels	$[(\pm 45)_2/90/0/45/90_2/-45/90_2/0_3/90/0/45/90/-45/90/0/45/90_2/-45/0/90/45/90_2/-45/0_3/90/0/90/45/90_2/-45/0/90/0_2/90/0_4/90/0_4/90/0/90/0_2/90_2/0_2/90/0/90/0_4/45/0_2/-45]_s$
Bottom skin panels	$[\pm 45/(90/0)_3/0_6]_s$

Table 9 Optimal design with 18 variables for the smeared-stiffness-based method

	n_0	n_{45}	n_{90}	n_0	n_{45}	n_{90}	
	Continuous			Rounded			Active constraints
Top skin panels							
Panel no. 16	30.20	12.54	24.56	30	13	25	——
Panel no. 17	18.69	20.53	12.10	19	21	12	——
Panel no. 18	24.43	5.40	8.92	24	6	9	Buckling
Bottom skin panels							
Panel no. 7	1.50	1.32	1.45	2	1	2	——
Panel no. 8	2.38	1.01	1.32	3	1	2	——
Panel no. 9	7.81	3.06	3.35	8	3	4	——
Buckling load factor	0.9960	——	——	1.0440	——	——	——
Total number of plies	448.82	——	——	460	——	——	——
Total number of plies [5]	465.63	——	——	464	——	——	——
Total volume, mm^3	1.671e7	——	——	1.710e7	——	——	——
Total volume [5], mm^3	1.732e7	——	——	1.726e7	——	——	——

Table 10 Stacking sequence of top and bottom skin panels for the optimal design with 18 variables[a]

Panel no.	Stacking sequence
	Top skin panels
16	$[(\pm 45)_2/(0_4/90/45/0/-45)_2/(0_4/90/45/90/-45)_2/90_2/0/(\pm 45)_3/(90/\pm 45)_4/(90_4/0_3)_3/90/0_2]_s$
17	$[(\pm 45)_2/(0_4/90/45/0/-45)_2/(0_4/90/45/90/-45)_2/90_2/0/(\pm 45)_3/(90/\pm 45)_4/(\pm 45)_8]_s$
18	$[(\pm 45)_2/(0_4/90/45/0/-45)_2/(0_4/90/45/90/-45)_2/90_2/0_4/90/0_2]_s$
	Bottom skin panels
7	$[\pm 45/90_2/0_2]_s$
8	$[\pm 45/90/0/90/0_2]_s$
9	$[\pm 45/90/0/90/0_2/(\pm 45)_2/0_4/90_2/0]_s$

[a]Buckling load factor is 1.019.

Table 11 Optimal design with 36 variables for the lamination-parameter-based method

	n_0	n_{45}	n_{90}	n_0	n_{45}	n_{90}			
	Continuous			Rounded			V_1^D	V_2^D	V_3^D
Top skin panels									
Panel no. 16	27.99	15.58	22.19	28	16	22	1.1268	1.0102	1.2132
Panel no. 17	25.59	12.54	19.40	26	13	19	1.1610	1.0086	1.3022
Panel no. 18	21.64	5.45	13.66	22	6	14	1.2398	1.0098	1.0982
Bottom skin panels									
Panel no. 7	4.39	1.30	1.28	5	1	1	1.3715	1.0579	0.7382
Panel no. 8	3.92	1.20	2.06	4	1	2	1.1144	1.0576	0.7906
Panel no. 9	7.48	1.72	2.68	8	2	3	0.8432	1.0485	0.9308
Buckling load factor	1.0039	——	——	1.0349	——	——	——	——	——
Total number of plies	456.68	——	——	464	——	——	——	——	——
Total number of plies [5]	465.63	——	——	464	——	——	——	——	——
Total volume, mm^3	1.704e7	——	——	1.726e7	——	——	——	——	——
Total volume [5], mm^3	1.732e7	——	——	1.726e7	——	——	——	——	——

Table 12 Lamination parameters of the panels with 36 variables

	$\tilde{V}_1^D$	$\tilde{V}_2^D$	$\tilde{V}_3^D$	Buckling load factor
Top skin panels				
Panel no. 16	1.1582	1.0070	1.2177	——
Panel no. 17	1.1801	1.0081	1.2030	——
Panel no. 18	1.2398	1.0139	1.0987	1.0337 (second buckling mode)
Bottom skin panels				
Panel no. 7	1.2630	1.0547	0.8958	——
Panel no. 8	1.2604	1.0547	0.8958	——
Panel no. 9	1.2084	1.0296	1.1270	0.9614 (first buckling mode)

Table 13 Stacking sequence of the panels with 36 variables

Panel no.	Stacking sequence
	Top skin panels
16	$[(\pm45)_2/(0_2/45/0_2/-45)_2/0_2/45/90/-45/(0/90)_2/0_2/90_3/0/90/0_3/90_3/0/90/45/90/-45/0/(0/90)_2/90_2/(90/0)_3/45/0/-45/(\pm45)_6/90_2/45/90/-45/(45/0/-45)_2]_s$
17	$[(\pm45)_2/(0_2/45/0_2/-45)_2/0_2/45/90/-45/(0/90)_2/0_2/90_3/0/90/0_3/90_3/0/90/45/90/-45/0/(0/90)_2/90_2/(90/0)_3/45/0/-45/(\pm45)_6]_s$
18	$[(\pm45)_2/(0_2/45/0_2/-45)_2/0_2/45/90/-45/(0/90)_2/0_2/90_3/0/90/0_3/90_3/0/90/45/90/-45/0/(0/90)_2]_s$
	Bottom skin panels
7	$[\pm45/0_4/90/0]_s$
8	$[\pm45/0_4/90_2]_s$
9	$[\pm45/0_4/90_2/45/90/-45/0_4]_s$

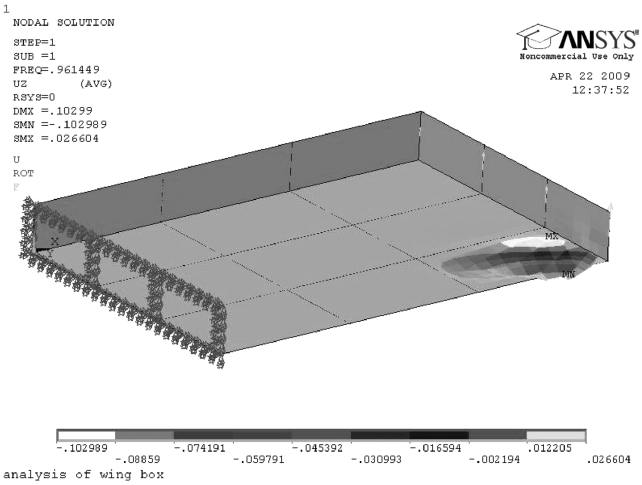

Fig. 7 First buckling mode.

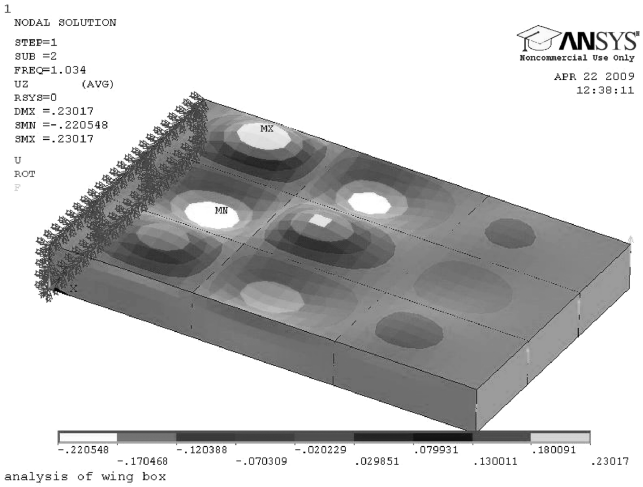

Fig. 8 Second buckling mode.

Table 14 Optimal design with 27 variables for the smeared-stiffness-based method

	n_0	n_{45}	n_{90}	n_0	n_{45}	n_{90}	
	Continuous			Rounded			Active constraints
Panel no. 10	26.21	15.25	15.61	26	16	16	——
Panel no. 11	21.90	15.49	13.46	22	16	13	——
Panel no. 12	21.21	6.79	9.22	21	7	9	buckling
Panel no. 13	25.40	7.12	6.86	25	8	7	buckling
Panel no. 14	30.71	16.24	13.91	31	17	14	——
Panel no. 15	34.46	18.38	17.70	34	19	18	——
Panel no. 16	28.57	15.48	16.46	29	16	16	——
Panel no. 17	29.83	11.65	15.11	30	12	15	——
Panel no. 18	24.95	5.45	10.72	25	6	11	——
Buckling load factor	0.9967	——	——	1.0032	——	——	——
Total number of plies	1171.9	——	——	1192	——	——	——
Total volume, mm^3	1.675e7	——	——	1.708e7	——	——	——

Table 15 Stacking sequence of top skin panels for the optimal design with 27 variables[a]

Panel no.	Stacking sequence
10	$[(\pm45)_2/(0_4/90/45/0/-45)_2/(0_4/90/45/90/-45)_2/90/0_4/(\pm45)_2/90/(90/\pm45)_4/(90/0_2)_2/(\pm45)_2/(\pm45/90)_2]_s$
11	$[(\pm45)_2/(0_4/90/45/0/-45)_2/(0_4/90/45/90/-45)_2/90_2/0_4/(\pm45)_2/90/(90/\pm45)_4/90/(\pm45)_4]_s$
12	$[(\pm45)_2/(0_4/90/45/0/-45)_2/(0_4/90/45/90/-45)_2/90/0_3/\pm45/90_2]_s$
13	$[(\pm45)_2/(0_4/90/45/0/-45)_2/(0_4/90/45/90/-45)_2/90/0_4/\pm45/0_3/\pm45]_s$
14	$[(\pm45)_2/(0_4/90/45/0/-45)_2/(0_4/90/45/90/-45)_2/90/0_4/(\pm45)_2/90/(90/\pm45)_4/(90/0_2)_2/(\pm45)_2/0_2/(\pm45/0)_3]_s$
15	$[(\pm45)_2/(0_4/90/45/0/-45)_2/(0_4/90/45/90/-45)_2/90/0_4/(\pm45)_2/90/(90/\pm45)_4/(90/0_2)_2/(\pm45)_2/(\pm45/90)_2/0_3/(\pm45)_2/0_3/45/0/-45/90_2/0]_s$
16	$[(\pm45)_2/(0_4/90/45/0/-45)_2/(0_4/90/45/90/-45)_2/90/0_4/(\pm45)_2/90/(90/\pm45)_4/(90/0_2)_2/(\pm45)_2/\pm45/90/\pm45/0/90/0_2]_s$
17	$[(\pm45)_2/(0_4/90/45/0/-45)_2/(0_4/90/45/90/-45)_2/90/0_4/(\pm45)_2/90/(90/\pm45)_4/(90/0_2)_2/0_2/90/0_2]_s$
18	$[(\pm45)_2/(0_4/90/45/0/-45)_2/(0_4/90/45/90/-45)_2/90/0_4/90_3/0_3/90]_s$

[a]Buckling load factors are 0.990 (first buckling mode, panel 9) and 0.994 (second buckling mode, panel 16).

Table 16 Optimal design with 54 variables for the lamination-parameter-based method

	n_0	n_{45}	n_{90}	n_0	n_{45}	n_{90}			
Panel no.	Continuous			Rounded			V_1^D	V_2^D	V_3^D
Panel no. 10	27.07	14.44	21.40	27	15	21	1.0978	1.0094	1.2446
Panel no. 11	25.34	12.85	19.08	25	13	19	1.1261	1.0086	1.2905
Panel no. 12	20.73	5.67	12.84	21	6	13	1.2319	1.0089	1.0736
Panel no. 13	20.70	5.66	12.84	21	6	13	1.2311	1.0087	1.0745
Panel no. 14	25.35	13.24	19.28	25	14	19	1.1189	1.0083	1.2596
Panel no. 15	27.66	15.70	22.04	28	16	22	1.0947	1.0096	1.2001
Panel no. 16	27.48	15.81	22.07	27	16	22	1.0987	1.0102	1.2013
Panel no. 17	25.56	13.49	19.36	26	14	19	1.1224	1.0082	1.2492
Panel no. 18	20.99	6.05	13.05	21	7	13	1.2243	1.0071	1.0460
Buckling load factor	1.0014	——	——	1.0213	——	——	——	——	——
Total number of plies	1177.32	——	——	1192	——	——	——	——	——
Total volume, mm^3	1.685e7	——	——	1.705e7	——	——	——	——	——

Table 17 Lamination parameters of the panels with 54 variables

Panel no.	$\tilde{V}_1^D$	$\tilde{V}_2^D$	$\tilde{V}_3^D$	Buckling load factor
10	1.1527	1.0080	1.1901	——
11	1.1685	1.0089	1.1774	——
12	1.2319	1.0143	1.0736	——
13	1.2319	1.0143	1.0736	——
14	1.1643	1.0086	1.1816	——
15	1.1457	1.0076	1.1934	——
16	1.1474	1.0077	1.1927	1.015
17	1.1623	1.0086	1.1833	——
18	1.2266	1.0135	1.0856	——

only the top skin is a designable area, the lamination parameters match reasonably well between the top level (Table 16) and the local level (Tables 17 and 18). The buckling load factor has decreased from 1.0213 at the top level to 1.015 at the local level. This shows that the lamination-parameter-based method works well for the optimization of laminated composite structures if a small difference between the lamination parameters from top-level optimization and those calculated in the local level can be produced. This can typically be achieved for realistic aircraft structures in which the number of plies is not too small so that blending does not prevent arriving at a good match of lamination parameters.

VIII. Conclusions

A bilevel composite optimization procedure was investigated and two approaches were examined for seeking the best stacking

Table 18 Stacking sequence of the panels with 54 variables

Panel no.	Stacking sequence
10	$[(\pm45)_2/0/(0_2/45/0/-45)_2/90/0_2/45/0_2/-45/(0/90)_2/90/0/90_2/45/90_2/-45/0_2/90/0_3/90_2/(90/0)_2/45/90_2/-45/90_4/0_2/45/0_2/-45/(\pm45)_6/0/90_2/0/\pm45]_s$
11	$[(\pm45)_2/0/(0_2/45/0/-45)_2/90/0_2/45/0_2/-45/(0/90)_2/90/0/90_2/45/90_2/-45/0_2/90/0_3/90_2/(90/0)_2/45/90_2/-45/90_4/0_2/45/0_2/-45/(\pm45)_5]_s$
12	$[(\pm45)_2/0/(0_2/45/0/-45)_2/90/0_2/45/0_2/-45/(0/90)_2/90/0/90_2/45/90_2/-45/0_2/90/0_3/90_2/(90/0)_2]_s$
13	$[(\pm45)_2/0/(0_2/45/0/-45)_2/90/0_2/45/0_2/-45/(0/90)_2/90/0/90_2/45/90_2/-45/0_2/90/0_3/90_2/(90/0)_2]_s$
14	$[(\pm45)_2/0/(0_2/45/0/-45)_2/90/0_2/45/0_2/-45/(0/90)_2/90/0/90_2/45/90_2/-45/0_2/90/0_3/90_2/(90/0)_2/45/90_2/-45/90_4/0_2/45/0_2/-45/(\pm45)_6]_s$
15	$[(\pm45)_2/0/(0_2/45/0/-45)_2/90/0_2/45/0_2/-45/(0/90)_2/90/0/90_2/45/90_2/-45/0_2/90/0_3/90_2/(90/0)_2/45/90_2/-45/90_4/0_2/45/0_2/-45/(\pm45)_6/0/90_2/0/\pm45/90/0/\pm45]_s$
16	$[(\pm45)_2/0/(0_2/45/0/-45)_2/90/0_2/45/0_2/-45/(0/90)_2/90/0/90_2/45/90_2/-45/0_2/90/0_3/90_2/(90/0)_2/45/90_2/-45/90_4/0_2/45/0_2/-45/(\pm45)_6/0/90_2/0/\pm45/90/\pm45]_s$
17	$[(\pm45)_2/0/(0_2/45/0/-45)_2/90/0_2/45/0_2/-45/(0/90)_2/90/0/90_2/45/90_2/-45/0_2/90/0_3/90_2/(90/0)_2/45/90_2/-45/90_4/0_2/45/0_2/-45/(\pm45)_6/0]_s$
18	$[(\pm45)_2/0/(0_2/45/0/-45)_2/90/0_2/45/0_2/-45/(0/90)_2/90/0/90_2/45/90_2/-45/0_2/90/0_3/90_2/(90/0)_2/\pm45]_s$

sequence of laminated composite wing structures with blending and manufacturing constraints.

In the smeared-stiffness-based method, the top-level optimization is performed using the assumption of homogenous laminates. A ply shuffling technique HyperShuffle is used at the local level without a need for solving an optimization problem. Manufacturing and general composite layup requirements are considered in the ply shuffling procedure. The obtained values of the buckling load factors for the case of two and six substructures do not violate the buckling constraints. For the case of nine substructures, a manual adjustment (adding layers) to the bottom skin layup following the blending and manufacturing requirements can prevent buckling.

In the lamination-parameter-based method, local optimization runs need to be performed to shuffle layers while matching the lamination parameter values passed from the top level. The stacking-sequence optimization in this level can also be done efficiently using a permutation GA, because it does not call any numerical simulation and only deals with calculating the lamination parameter values by simple formulas. Once the stacking sequence is determined that satisfies the blending and manufacturing requirements, no buckling analysis needs to be performed if the target values of the lamination parameters, passed from the top level, were kept. Based on three cases in this paper, it seems difficult to match the lamination parameters from the top level while considering ply continuity for a small number of plies in the bottom skin of the laminated composite wing box. Such problems did not occur for a more realistic case of a larger number of plies, as in the top skin.

References

[1] Gurdal, Z., Haftka, R. T., and Hajela, P., *Design and Optimization of Laminated Composite Materials*, Wiley, New York, 1999.

[2] Schmit, L. A., and Farshi, B., "Optimum Laminate Design for Strength and Stiffness," *International Journal for Numerical Methods in Engineering*, Vol. 7, 1973, pp. 519–536. doi:10.1002/nme.1620070410

[3] Stroud, W. J., and Agranoff, N., "Minimum Mass Design of Filamentary Composite Panels Under Combined Loads: Design Procedure Based on Simplified Equations," NASA TN D-8257, 1976.

[4] Nemeth, M. P., "Importance of Anisotropy on Buckling of Compression-Loaded Symmetric Composite Plates," *AIAA Journal*, Vol. 24, 1986, pp. 1831–1835. doi:10.2514/3.9531

[5] Liu, B., Haftka, R. T., and Akgun, M. A., "Two-Level Composite Wing Structural Optimization Using Response Surface," *Structural and Multidisciplinary Optimization*, Vol. 20, 2000, pp. 87–96. doi:10.1007/s001580050140

[6] Liu, B., Haftka, R. T., and Trompette, P., "Maximisation of Buckling Loads of Composite Panels Using Flexural Lamination Parameters," *Structural and Multidisciplinary Optimization*, Vol. 26, 2004, pp. 28–36. doi:10.1007/s00158-003-0314-7

[7] Tsai, S. W., Halpin, J. C., and Pagano, N. J., *Composite Materials Workshop*, Technomic, Westport, CT, 1968, pp. 233–253.

[8] Fukunaga, H., and Hirano, Y., "Stability Optimization of Laminated Composite Plates Under In-Plane Loads," *Proceedings of the 4th International Conference on Composite Materials*, 1982, pp. 565–572.

[9] Miki, M., "Material Design of Composite Laminates with Required In-Plane Elastic Properties," *Proceedings of the 4th International Conference on Composite Materials*, 1982, pp. 1725–1731.

[10] Fukunaga, H., and Chou, T. W., "On Laminated Configurations for Simultaneous Failure," *Journal of Composite Materials*, Vol. 22, 1988, pp. 271–286. doi:10.1177/002199838802200305

[11] Fukunaga, H., and Sekine, H., "Optimum Design of Composite Structures for Shape, Layer Angle and Layer Thickness Distributions," *Journal of Composite Materials*, Vol. 27, 1993, pp. 1479–1492. doi:10.1177/002199839302701504

[12] Diaconu, C. G., Sato, M., and Sekine, H., "Feasible Region in General Design Space of Lamination Parameters for Laminated Composites," *AIAA Journal*, Vol. 40, 2002, pp. 559–565. doi:10.2514/2.1683

[13] Herencia, J. E., and Weaver, P. M., "Local Optimization of Long Anisotropic Laminated Fibre Composite Panels with T Shape Stiffeners," 47th AIAA SDM Conference, AIAA Paper 2006-2171, Newport, RI, May 2006.

[14] Herencia, J. E., Haftka, R. T., Weaver, P. M., and Friswell, M. I., "Optimization of Anisotropic Composite Panels with T-Shaped Stiffeners Using Linear Approximations of the Design Constraints to Identify Their Stacking Sequence," *Proceedings of 7th ASMO UK/ISSMO Conference*, 2008.

[15] Herencia, J. E., Haftka, R. T., Weaver, P. M., and Friswell, M. I., "Lay-Up Optimization of Composite Stiffened Panels Using Linear Approximations in Lamination Space," *AIAA Journal*, Vol. 46, 2008, pp. 2387–2391. doi:10.2514/1.36189

[16] Bloomfield, M. W., Herencia, J. E., and Weaver, P. M., "Enhanced Two-Level Optimization of Anisotropic Laminated Composite Plates with Strength and Buckling Constraints," *Thin-Walled Structures*, Vol. 47, 2009, pp. 1161–1167. doi:10.1016/j.tws.2009.04.008

[17] Kristinsdottir, B. P., Zabinsky, Z. B., Tuttle, M. E., and Neogi, S., "Optimal Design of Large Composite Panels with Varying Loads," *Composite Structures*, Vol. 51, 2001, pp. 93–102. doi:10.1016/S0263-8223(00)00128-8

[18] Liu, B., and Haftka, R. T., "Composite Wing Structural Design Optimization with Continuity Constraint," 42th AIAA SDM Conference, AIAA Paper 2001-1205, Seattle, WA, 2001.

[19] Soremekun, G. A., Gurdal, Z., Kassapoglou, C., and Toni, D., "Stacking Sequence Blending of Multiple Composite Laminates Using Genetic Algorithm," *Composite Structures*, Vol. 56, 2002, pp. 53–62. doi:10.1016/S0263-8223(01)00185-4

[20] Seresta, O., Gurdal, Z., Adams, D. B., and Watson, L. T., "Optimal Design of Composite Wing Structures with Blended Laminates," *Composites, Part B*, Vol. 38, 2007, pp. 469–480. doi:10.1016/j.compositesb.2006.08.005

[21] Ijsselmuiden, S. T., Abdalla, M. M., Seresta, O., and Gürdal, Z., "Multi-Step Blended Stacking Sequence Design of Panel Assemblies with Buckling Constraints," *Composites, Part B*, Vol. 40, 2009, pp. 329–336. doi:10.1016/j.compositesb.2008.12.002

[22] Liu, W., and Butler, R., "Optimum Buckling Design of Composite Wing Cover Panels with Manufacturing Constraints," 48th AIAA SDM Conference, AIAA Paper 2007-2215, Honolulu, HI, April 2007.

[23] Liu, W., and Krog, L., "A Method for Composite Ply Layout Design and Stacking Sequence Optimisation," *Proceedings of 7th ASMO UK/ ISSMO Conference*, Bath, England, U.K., 2008.

[24] Toropov, V. V., Jones, R., Willment, T., and Funnell, M., "Weight and Manufacturability Optimization of Composite Aircraft Components Based on a Genetic Algorithm," *Proceedings of 6th World Congress of SMO*, 2005.

[25] Jones, R. M., *Mechanics of Composite Materials*, 2nd ed., Taylor and Francis, New York, 1999.

[26] Zhou, M., and Fleury, R., "Optimization of Composite Structures—Understanding and Meeting the Challenges," *Altair Composite Seminar*, Altair Engineering, Ltd., Royal Leamington Spa, England, U.K., 2007.

[27] Altair OptiStruct, Software Package, Ver. 9.0, Altair Engineering, Inc., Troy, MI, 2008.

[28] ANSYS, Software Package, Ver. 11, ANSYS, Inc., Canonsburg, PA, 2007.

[29] Schramm, U., "Altair's Product Direction-Solver Technologies," *European HyperWorks Technology Conference 2007*, Berlin, Oct. 2007.

[30] Diaconu, C. G., and Sekine, H., "Layup Optimization for Buckling of Laminated Composite Shells with Restricted Layer Angles," *AIAA Journal*, Vol. 42, 2004, pp. 2153–2163.
doi:10.2514/1.931

[31] Bloomfield, M. W., Diaconu, C. G., and Weaver, P. M., "On Feasible Regions of Lamination Parameters for Lay-Up Optimization of Laminated Composites," *Proceedings of the Royal Society of London, Series A: Mathematical and Physical Sciences*, Vol. 465, No. 2104, 2009, pp. 1123–1143.
doi:10.1098/rspa.2008.0380

[32] Niu, M. C. Y., *Composite Airframe Structures, Practical Design Information and Data*, Conmilit Press, Ltd., Hong Kong, 1992.